2D FAN TOMOGRAPHIC RECONSTRUCTION OF FLAME CHEMILUMINESCENT EMISSION

Armando Caldeira-Pires
Dept of Mechanical Engineering
Faculty of Engineering – University of Brasilia
70910-900 Brasilia DF Brazil
armandcp@unb.br

Bruno Rodrigues Roque
Dept of Mechanical Engineering
Faculty of Engineering – University of Brasilia
70910-900 Brasilia DF Brazil

Marcelo Alves Araujo
Dept of Mechanical Engineering
Faculty of Engineering – University of Brasilia
70910-900 Brasilia DF Brazil

Abstract. *This paper reports an on-going work addressing the development and implementation of an algorithm for tomographic reconstruction of reacting flows emissions to be employed as a diagnostic tool of combustion processes, by using images, or projections, obtained from digital cameras. The algorithm is based on the deconvolution of a finite number of two-dimensional path integrated measurements of radiative flame intensity. In this context, image reconstruction algorithms implemented on computed tomography systems require that projection data be available for evenly spaced view surrounding the object. However, in most practical combustion applications of interest, the projection data are available only through a limited angle or number of views, mainly due by geometric constraints in the scan structure of the imaging system itself. This situation, referred to as the limited-view problem, has led to the development of specialized algorithms. This work adopts an innovative approach by introducing a 2D fan methodology where an element of a CCD camera image array integrates radiation along an optical path which is divergent in two dimensions. It is assumed that the extra computational effort represented by this approach will result in more accurate, both intensity and spatially, reconstructed images from flame chemiluminescence emissions.*

Keywords*: Combustion, Diagnostic Methods, Tomographic Reconstruction, SART, 2D Fan*

1. Introduction

An exhaustive analysis of combustion processes is a pre-requisite to reduce pollutant emissions, for fuel economy, for the optimization of burner performance and for on-line control purposes. Local point measurements give only scarce information to characterize the spatially distributed and time-dependent combustion phenomena of complex reactive fluid dynamical processes. Otherwise, large array sensors like CCD arrays provide us with a huge amount of information, which, combined with image processing techniques as well as pattern-recognition methods, give a much higher potential for the analysis of such processes and have the attraction of an optical measurement technique, with its non-contact and non-intrusive features.

A flame can be modeled as a set of layers, within which all scalar properties are constant, by the method of the onion peeling. The section area of the flame is calculated by the Algebraic Reconstruction Technique (ART). This method minimizes the errors associated to the inversion of Abel's transform along the axis of symmetry. This method has been developed during the last years by several authors (Caldeira-Pires, 2001, Caldeira-Pires et al., 2002, Correia et al., 2000, Correia et al., 2002) and a deep analysis is reported by Correia (2001).

This paper reports an on-going work addressing the development and implementation of a diagnostic tool of combustion processes. This experimental method is based on a tomographic reconstruction algorithm to be applied on the reconstruction of the locus and of the intensity of flame chemiluminescence emissions projections, obtained from digital cameras at specific wavelengths. The algorithm is based on the deconvolution of a finite number of two-dimensional path integrated measurements of radiative flame intensity.

Moreover, image reconstruction algorithms implemented on computed tomography systems require that projection data be available for evenly spaced view surrounding the object. In most practical combustion applications of interest, the projection data are available only through a limited angle or number of views, mainly due by geometric constraints in the scan structure of the imaging system itself. This situation, referred to as the limited-view problem, has led to the development of specialized algorithms.

In this sense, this work innovates by adopting a 2D fan approach of light collection, where the CCD array integrates radiation along a two-dimensional divergent optical path. Actually, a first movement toward the use of this technique applied to flame characterization was reported by Costa and Caldeira-Pires (1999), based on a former report of Clarck et al. (1989), and this paper hereinafter presents recent developments on this matter.

2. Tomographic Reconstruction

The tomographic reconstruction consists in the characterization of the internal structure of an object based on one or more projections or images.

In 1917, J. Randon, for the first time, hit upon a formula for this calculation, which became known as the "Randon Transformed". It was optimized and applied later to the radio astronomy by Bracewell (1956).

Over the following decades, computerized tomography has been increasingly employed as a very useful technique in multidisciplinary applications, ranging from modern medicine using X-ray computerized tomography and Nuclear Magnetic Resonance to the study of materials such as soil and flames.

Traditionally cameras are multislice devices, which image and reconstruct a three-dimensional distribution as a set of parallel two-dimensional sections. This approach greatly simplifies the reconstruction of the data by decomposing a three-dimensional problem into a set of two-dimensional problems.

Tomographic reconstruction of local flame scalar properties is based on the deconvolution of a finite number of two-dimensional path integrated measurements of radiative flame intensity. Usually, the algorithm developed for axissymmetric systems assumed parallel optical path geometry. For the non-axissymmetric reconstruction algorithms, the optical paths are assumed to be divergent in a single dimension (fan geometry). However, in reality an element of a CCD camera image array integrates radiation along an optical path, which is divergent in two dimensions (2D fan). The difference between these various approaches is illustrated in Fig. 1.

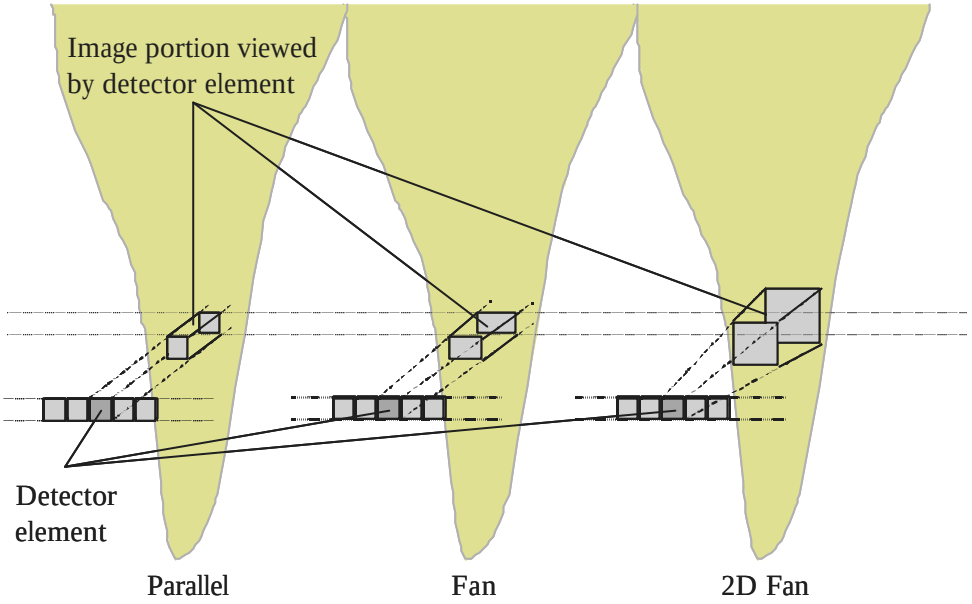

Figure 1. Schematic representation of the optical path approaches.

The geometrical constraints of the camera may result in projections that are truncated, and hence only partially measured. Most algorithms that have being proposed for three-dimensional reconstruction are extensions of two-dimensions algorithms for which all projections are assumed to be complete. The errors associated with the parallel path approach increase for lower distances between the detector and the object centre and for increased fan divergence angles.

2.1. Theoretical development

The reconstruction of non-axissymmetric flames requires the acquisition of a larger number of projections and dedicated algorithms. Integral methods, as those based on Radon's transform, require a large number of projections (more than 100, generally), taken from uniformly spaced angles around the object. Some studies concluded that improved performance is achieved using algebraic methods (ART) that are able to reconstruct a 3D object correctly from a limited number of projections, typically below 5. Therefore, considering that on real-scale non-laboratorial facilities optical access is limited, the study of non-axissymmetric systems was undertaken using algebraic techniques.

ART are based on a representation of the projection line integrals as discrete ray sums, the image reconstruction are based on iterative procedures. The problem of tomographic reconstruction using an iterative algebraic technique becomes one of solving a system of linear equations as the Eq. 1:

$$P_j = \sum_{i=1}^{R^2} A_{ij} \cdot F_i \qquad (1)$$

In Eq. 1, F_i represents the unknown image function values, on a sampling grid of size $R \times R$ and the solution is expressed in terms of the given projection data P_j. The subscript j represents the ray index among J rays within all projections. The summation coefficients, A_{ij}, correspond to the intersection areas between each ray and the sampling grid.

Typically, the reconstruction process is performed line after line, admitting that the optical paths are flat. However, when light is collected by a camera, the optical paths are divergent (fan), according to the divergence angle of the lenses on the optical data collection system. As a consequence, in order to improve the accuracy of the sensor, in the present algorithm, the approach followed was to assume fan geometry in one dimension, for the geometric correlations between projection detector elements and the spatial grid surrounding the object (evaluation of A_{ij}).

Algebraic reconstruction techniques consist on an iterative method for solving equation systems, where an estimate, $F_i^{(r)}$, of the image function, F_i, is updated to satisfy a particular ray sum. In this iterative procedure, the new estimate, $F_i^{(r+1)}$, is determined from the previous after *'r'* steps, by an update-correction procedure which is defined by Eq. 2:

$$F_i^{(r+1)} = F_i^{(r)} + \lambda . A_{ij} \left[\frac{P_j - \sum_i A_{ij} F_i^{(r)}}{\sum_j A_{ij}^2} \right] \qquad (2)$$

In this equation, the difference $P_j - \sum A_{ij} F_i^{(r)}$ represents the error between the correct projection value, P_j, and the re-projection of the image estimate, F_i, after *'r'* iterations. $\sum_j A_{ij}^2$ is a normalization factor, and the correction (the term between square brackets) is backdistributed to the image samples, F_i, along the ray according to the weighing coefficients, A_{ij}. Relaxation factor (l) can be varied between steps and may be chosen in the range 0.0 to 2.0, in order to improve convergence.

Improved reconstructed images can be obtained by combining correction terms from all rays within a particular projection before the image function is updated. The approach, initially derived by Andersen and Kak (1984), is referred to as the simultaneous algebraic reconstruction technique, SART, and leads to an update-correction strategy defined as:

$$F_i^{(r+1)} = F_i^{(r)} + \lambda \frac{\sum_j A_{ij} \Delta_j}{\sum_j A_{ij}}, \text{ where } \quad \sum_j A_{ij} \Delta_{ij} = \sum_j \left[A_{ij} \frac{P_j - \sum_i A_{ij} F_i^{(r)}}{\sum_i A_{ij}} \right] \qquad (3)$$

The present work follows that reported by Correia (2001), where the convergence criteria for the iterative process of reconstruction is defined by Eq. 4, which states that the algorithm converges when, among the N points which constitute the spatial grid containing the object, a percentage equal or higher than μ, the grid convergence factor, has converged. Convergence of an individual point is said to occur when the absolute value of the difference between the values of the reconstructed function on that point, for two consecutive iterations, is below δ, the convergence factor.

$$\sum_N \left\{ i : i \le N \wedge \left| F_i^{(r+1)} - F_i^{(r)} \right| \le \delta \right\} \ge \mu \cdot N \qquad (4)$$

2.2. Computer implementation

The computer implementation of the SART algorithm required the development of some routines in C++ language, that is sufficiently spread out and offers good routines to work with images, graphical interfacing, besides being a object-oriented program language that makes possible capsule the font code such as the real things. The non-axissymmetric reconstruction problem is in essence a very intensive process in computational terms. Even for a limited number of projections, which is always higher than 2 and normally above 50 (except for algebraic reconstruction algorithms), the algorithms require the manipulation of large arrays and intricate calculations, involving the various projection elements and the nodes of the 2D spatial grid. Here, the reconstruction process was developed to allow the reconstruction of the flame structure based on sets of few projections.

Fig. 2 illustrates the fundamental steps of the procedure implemented to test the SART algorithm, making use of a flowchart that describes the sequence of actions on the reconstruction process for non-axissymmetric objects.

With the exception of the evaluation of the original test function and the projection (Fo_i and P_j), which are condensed in a singular C++ language program, grouped inside the dashed line in the flowchart in Fig. 2, all the remaining operations correspond to individual programs. This program is displayed in a friendly graphical interfacing that offers facilities in the manipulation and display of the results.

2.2.1. Area array mapping

These routines consists on the mapping of the A_{ij} array which, involves the evaluation of the areas of intersection between each ray leaving a given projection element and each spatial grid element or node. This routine encompassed several steps, presented in the flowchart in Fig. 3.

The input parameters for this routine can be divided into three main groups: geometric parameters, hardware characteristics and the projection angles. The first are related to basic tomographic variables such as the number of nodes and the number of projection elements. The second set characterizes acquisition hardware parameters and is related to geometric properties of the detector. In the present context, only two of these parameters were considered: the detector divergence angle and the detector relevant dimension. For a CCD detector, these parameters correspond to the divergence angle of the lenses and the CCD height. It can be argued that the number of projection elements (pixel) may also constitute an acquisition parameter, since the projection can be resized in the processing stages, either through interpolation or by selecting a specific detector array area, it was considered more adequate to include it in the geometry parameters. The projection angles identify the region around the object for which projections were retrieved.

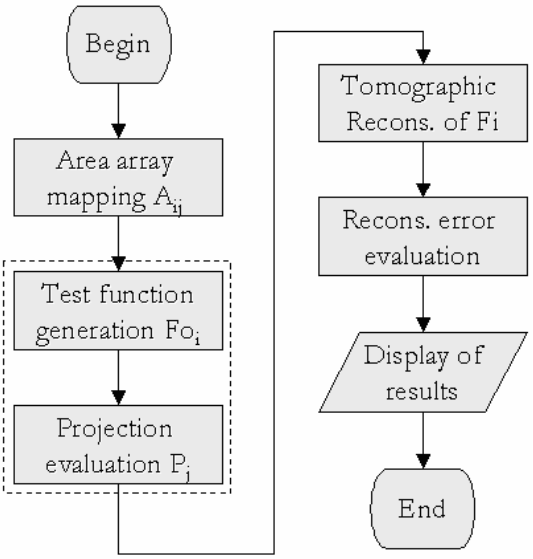

Figure 2. Flowchart of the computational procedure developed for the testing of the implemented non-axissymmetric tomographic reconstruction algorithm.

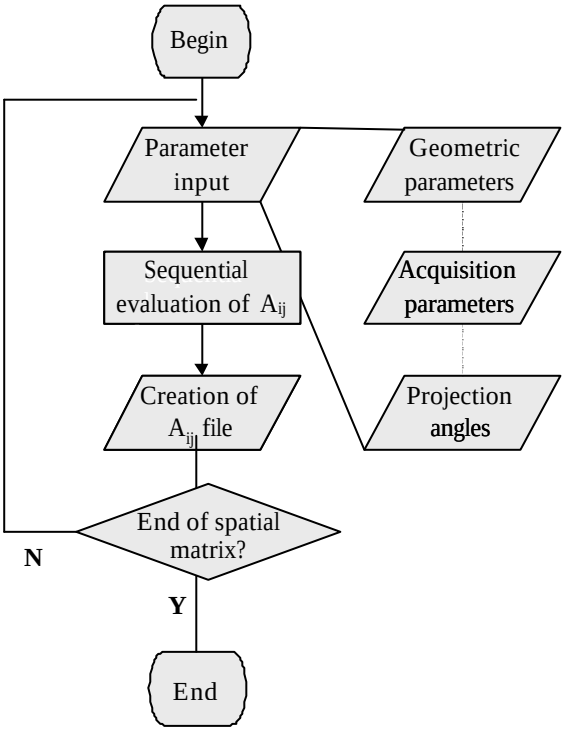

Figure 3. Flowchart of the area array mapping computational routine.

In the first step, the user define the distance of the CCD to the spatial grid, the number of integration points (the number of step in the numerical integration), the divergence angle, the width of the CCD, in meters and in pixels, in a dialog box, show in Fig. 4.

The value of the geometric parameters and the projection angles are introduced in the group box 1. In this box are acquired, respectively, the number of elements in the spatial grid, the projection angles, and the width of the spatial grid. The dimensions of the spatial grid, in meters, is based on the detector divergence angle and width, and on the distance from the detector to the centre of the spatial grid, assuming that the first and last ray encompass the limits of the grid.

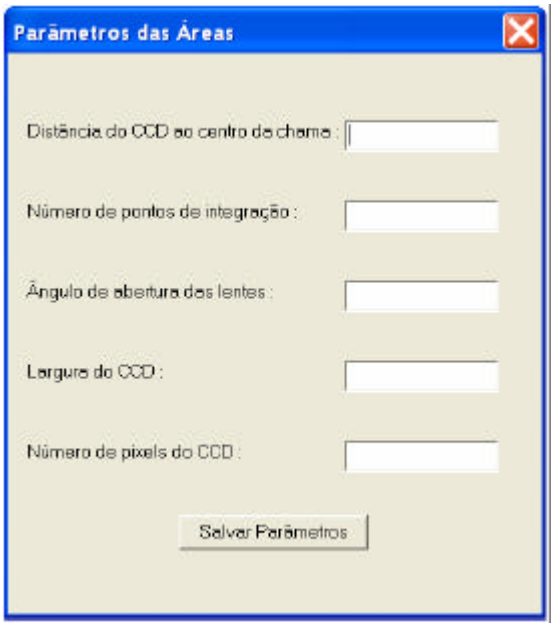

Figure 4. Dialog box for area array mapping.

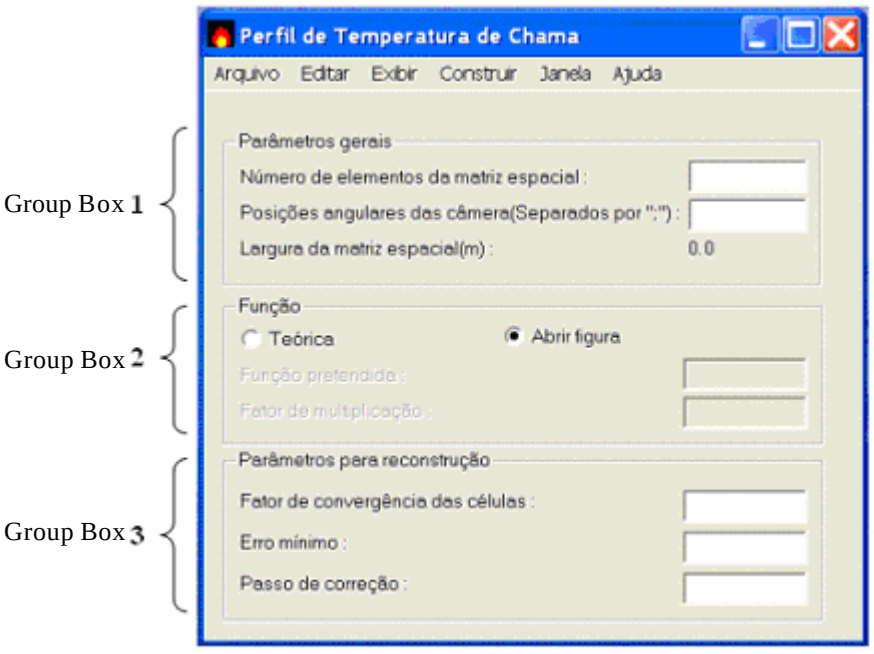

Figure 5. Main window in that introduces the parameters to the tomographic reconstruction.

The computation of the values of A_{ij} is carried out in sequential order, as represented in the flowchart in Fig. 3. For each spatial grid element, i, the geometric intersection with each ray, j, is verified. If an intersection is identified (the ray crosses the cell), the area of intersection is computed numerically by dividing the cell into a constant number of rectangles and summing the corresponding areas. Naturally, since each ray only crosses a few elements on the spatial grid, most of the A_{ij} values will be zero. Fig. 6a and b schematically represent this process.

The final step of this routine involves saving the A_{ij} array on a file. A relevant aspect concerning this task is the fact that the array often turns out to be reasonably large and produce a file of very significant size, for example, for 4 projections, 25 pixels and a 15x15 node spatial grid, a 2.2 MB ASCII file is produced.

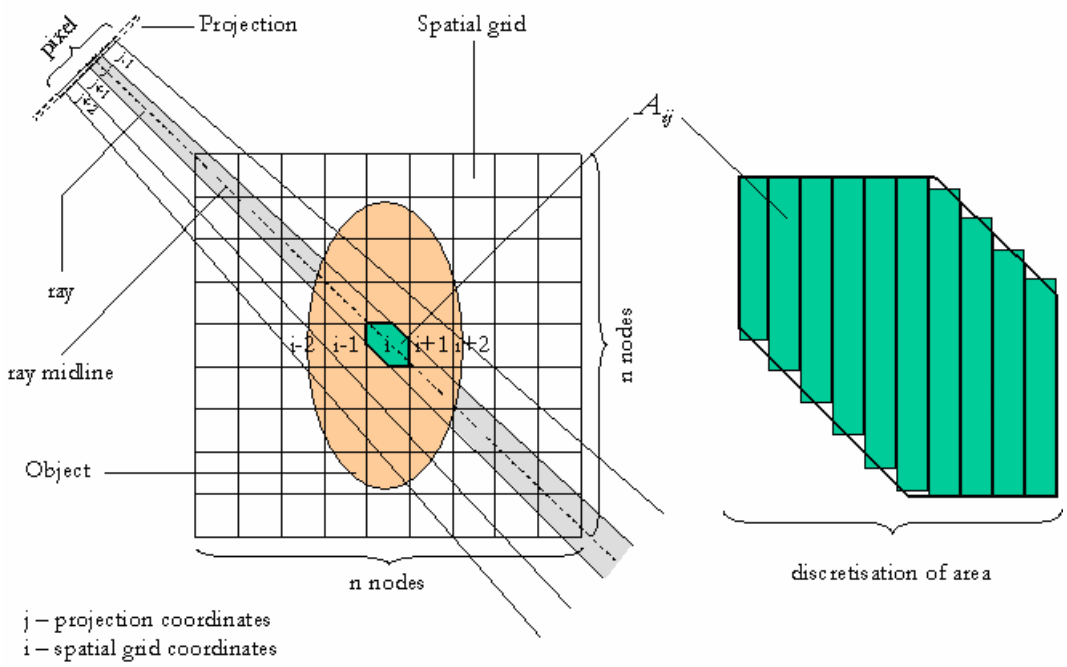

a) b)

Figure 6. Schematic description of the mapping the area array
a) Intersection of a projection ray and a given spatial grid element, and;
b) evaluation of intersection areas with a rectangle discretisation procedure.

2.2.2. Volume array mapping (2D Fan)

This innovation is at the tomographic reconstruction, the area array mapping is being improved to a 2D fan. The program calculates the volume of all rays that intersect each cell Fig. 7, rather than the area.

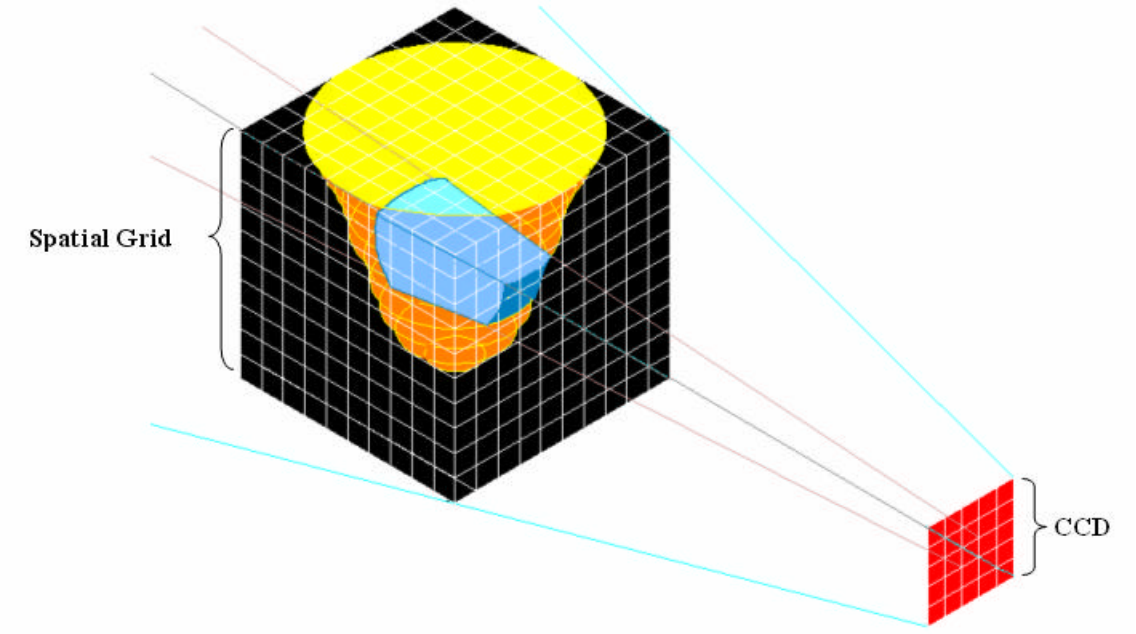

Figure 7. Schematic description of the mapping volume array.

For a cell (spatial grid element) the program verifies if any ray (projection coordinate) intersects the cell, it means that all pixels are verified for each cell. So if there are j pixels at the CCD it will verify j^2 pixels, it is the square of the pixels that are verified at the area array. And there are n t imes more nodes (cells) at the spatial grid to verify.

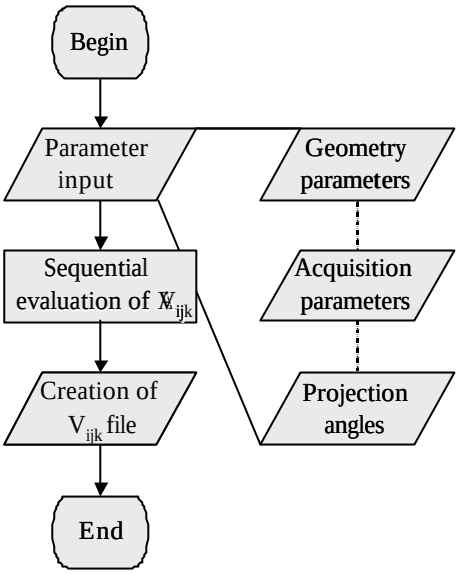

Figure 8. Flowchart of the volume array mapping routine.

If the intersection happens, then the volume is computed similar to the area array. The difference is that the constant rectangles have a height that is calculated for each one.

Because of the size that the matrix can get, the value of the volume is directly saved into a file. This improvement made the program faster and lighter (the areas where saved in an array that uses a lot of memory). But the size of the file is much bigger then area array. For the same example, 4 projections (cameras), 25x25 pixels and 15x15x15 node spatial grid produced a 64.4 MB text (ASCII) file (less than 25(due to all CCD lines)*15(due to all spatial grid layers) times 2.2Mb, the aforementioned memory requirement for the area mapping approach).

2.2.3. Evaluation of test functions and their projections

Figure 9 illustrates the essential phases of this routine. The projection generation program includes a subroutine, which allows the generation of up to nine different test functions.

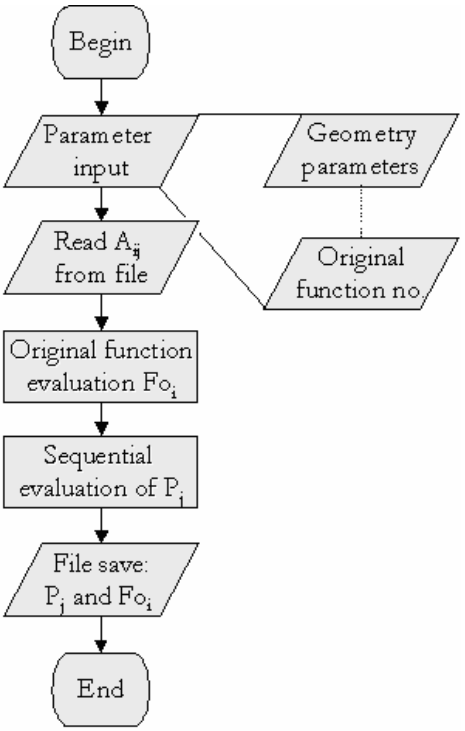

Figure 9. Flowchart of the computational routine for the evaluation of the original test function and the projections.

Once the input parameters are established and the A_{ij} values from the previously generated file are read, the routine proceeds by evaluating the value of the original mathematical test function on every point of the spatial grid by applying the exact equation for Fo_i. The selection of the function and the multiplication factor are introduced in the group box 2 of the window in the Fig. 6. Finally the projection assembly is simply done by performing the direct integration process, following Eq. 1. The program terminates by storing the projection and original function on disk files.

2.2.4. SART

The final steps on the reconstruction process consist on performing the tomographic reconstruction using the modified SART. The parameters for the tomographic reconstruction are introduced in the group box 3 in the Fig. 5. The first parameter is the grid convergence factor (μ), the second is the relaxation factor (λ), and the last is the convergence factor (δ). The routine illustrated in Fig. 10 is the tomographic reconstruction which is basically a direct computational implementation of the iterative algorithm described by Eq. 3, with a convergence criteria defined by Eq. 4.

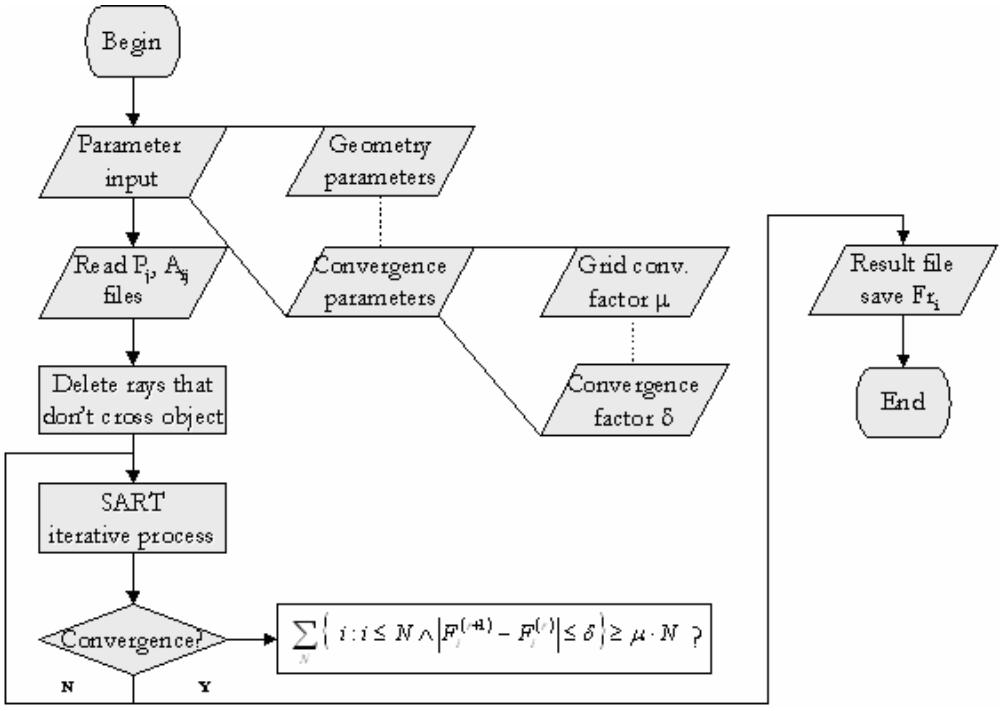

Figure 10. Flowchart of the modified SART reconstruction algorithm computational routine.

Two other aspects should be mentioned concerning this program. First, as represented on the flowchart in Fig. 10, prior to the beginning of the iterative process, there is a subtask dedicated to deleting rays that do not cross the object. This is performed in order to reduce processing time and improve the reconstruction quality by withdrawing from the reconstruction process rays and spatial grid elements where the object is clearly not present. Through this process, a smaller array A_{ij} is obtained and the number of projection elements for processing is also reduced.

3. Further developments

Up to now the work here reported presents the development of the 2D fan tomographic reconstruction algorithm that provides the main data processing framework to the analysis of combustion systems. The project's next steps include the computational implementation of these algorithms, and their validation with mathematical test functions, both to the area as well to the volume mapping approach.

A final step will be the experimental implementation of this diagnostic technique and its validation on laboratorial combustion systems. This will encompass the definition of the flame characteristics, premixed and non-premixed, as well as those issues related with the assembly of the imaging sensor, namely in every aspect related to the data collection system and the combustion systems.

The measurements performed with the optical sensor will include the acquisition of chemiluminescence emissions from main free radical species of the hydrocarbon chemical kinetics oxidation process, namely those related with carbon oxidation (•CH-431nm, •C2-516nm, •OH-308nm) and with nitrogen oxidation (•CN-388nm, •NH-355nm, •NO-226nm). These results will be compared with data obtained using "conventional" intrusive techniques, for instance combustion gases sampling and analysis.

4. Acknowledgement

Financial support has been provided by the Eletronorte Research and Development Funding Program, in the context of the Electrical Energy Sector Fund, under the contract nº Eletronorte 4500013171.

5. References

Andersen, A. H., Kak, A. C., 1984, "Simultaneous Algebraic Reconstruction Technique (SART): A Superior Implementation of the ART Algorithm", School of Electrical Engineering, Purdue University, pp 81-94.

Caldeira-Pires, A., 2001, "Free Radical Imaging Techniques applied to Hydrocarbon Flames Diagnosis", J. of Thermal and Fluid Sciences, **10(2**), pp. 132-145.

Caldeira-Pires, A., Correia, D.P., Lacava, P., Maia, P. and Heitor, M.V., 2002, "Influence of Burner-port Geometry in Hydrocarbon Oxidation and NOx Formation Mechanisms in Methane/Air Flames", Fuel, **81**, pp. 771-783.

Clarck, R., Townsend, D., Defrise, M., 1989, "An Algorithm for Three-Dimentional Reconstruction Incorporating Cross-Plane Rays", IEEE.

Correia, D. D. A. P., 2001, "Development and Implementation of Tomographic Reconstruction Techniques for the Diagnostic of Combustion Flows", Ph.D. Thesis on Mechanical Enginnering, Technical University of Lisbon, pp. 1-85.

Correia, D. P., Ferrão, P. and Caldeira-Pires, A., 2000, "Flame 3D Tomography Sensor for In-Furnace Diagnostics", 28th (Int.) Symposium on Combustion, Edinburgh, UK, 2000.

Correia, D.P., Ferrão, P. and Caldeira-Pires, A., 2001, "Advanced 3D Emission Tomography Flame Temperature Sensor", Science Combustion and Technology, **163**, pp. 1-24.

Costa, F. and Caldeira-Pires, A., 1999, "Efects of the Optical Path Divergence on the Flame Emission Tomographic Reconstruction (In Portuguese)", 15th Brazilian Congress of Mechanical Engineering, Aguas de Lindoia – SP, 1999.

Ribeiro, G. C., Cruvinel, P. E., 1997, "Tridimentional Image Reconstruction Method Based on the Modifield Algebraic Reconstruction Technique and B-spline Interpolation", IEEE, pp. 111-118.

Teixeira, R. C., 2001, "Tomographic Technique appllied to Flame Temperature Characterization (In Portuguese)", Master Thesis on Mechanical Engineering, Univesity of the State of São Paulo, Guaratinguetá, Brazil, pp 18-58.

5. Copyright Notice